Theoretical Studies on Inclusion Complexes of Cyclodextrins

M. Nagaraju and G. Narahari Sastry*

Molecular Modeling Group, Organic Chemical Sciences-I, Indian Institute of Chemical Technology, Tarnaka, Hyderabad 500 007, AP, India

Received: April 29, 2009; Revised Manuscript Received: June 17, 2009

Quantum chemical calculations and molecular dynamics simulations are carried out to study the host−guest inclusion complexes of cyclodextrins (α-, *β*-, and *γ*-CDs) with small guest molecules such as H_2O, NH_3, NH_4^+, C_6H_6, and bisimidazolyl compounds. The uptake ability of the CDs to accommodate the small molecules inside the cavity is examined by the sequential addition of 10 molecules of water or ammonia using the semiempirical (PM3) method. In the case of benzene, this was done up to six molecules. PM3 calculations indicate that α-, *β*-, and *γ*-CD can accommodate three, seven, and nine water molecules, respectively. In the case of NH_3 as guest molecule, α-, *β*-, and *γ*-CDs can accommodate up to two, five, and six molecules, respectively. Semiempirical calculations indicate that two benzene molecules can be accommodated in the α-CD cavity, whereas *β*- and *γ*-CD cavities adopt three and four benzene molecules, respectively. Molecular dynamics simulations were carried out for 1.0 ns on benzene and bisimidazolyl complexes of CDs in explicit solvent (TIP3P water model). The interaction energies calculated by the MM/PBSA method reveal that ligand 1,6-bis(imidazol-l-lyl) hexane (**B**) and 1,4-bis(imidazol-l-lylmethyl) benzene (**C**) molecules prefer to form 1:1 complexes with α-, *β*-, and *γ*-CDs. However, **C** preferentially forms 1:2 complexes with α-CDs. Ligands 1,10-bis(imidazol-l-lyl) decane (**A**) and 4,4′-(bis(imidazol-l-ylmethylene))biphenyl (**D**) form 1:2 complexes with α-, *β*-, and *γ*-CDs in head-to-head (HH) orientation of CDs. The stability of inclusion compounds depends on the type of CD and the physicochemical properties of the involved guest. Both of these methods (semiempirical and MD simulations) reveal that *β*-CDs form more stable complexes compared with α- and *γ*-CDs with **C**, **D**, NH_4^+, and C_6H_6, whereas α-CD forms more stable complexes with **A** and **B**.

Introduction

Host−guest phenomena concerning inclusion complexes that are formed through noncovalent interactions between small molecules have important applications in supramolecular chemistry, biology, and pharmacy.[1,2] CDs are cyclic oligosaccharides of α-(1,4) linked D-glucose units in a ring formation containing a relative hydrophobic central cavity and a hydrophilic outer surface (Figure 1). The most common CDs are α-, *β*-, and *γ*-CDs, which are formed by six, seven, and eight glucose units, respectively. These CDs generate a toroidal/hollow truncated cone structure because of the $^4C_1$ chair conformation of the sugar units.[3] The depth of the CD cavity is 7.9 Å, where bottom and top diameters are 4.7 and 5.3 Å for α-CD, 6.0 and 6.5 Å for *β*-CD, and 7.5 and 8.3 Å for *γ*-CD, respectively.[4] In recent years, rotaxenes and pseudorotaxanes have been the object of increased interest on account of their potential to serve as molecular devices, molecular machines, and functional materials.[5a,b] Pseudorotaxanes are a type of supramolecular assembly that consists of a cyclic molecule that acts as the wheel and is the host and a threadlike molecule that acts as the axle and is the guest.[5c,d] Among the suitable macrocycle candidates, cyclodextrins have been successfully used as hosts to form rotaxanes with linear, polymeric chains.[5e,f] The stoichiometries for most of the CD/substrate inclusion complexes are 1:1[6] or 2:1,[7−10] although some cases of 2:2 stoichiometries have also been detected.[11]

Computational chemistry techniques have been widely used to study the host−guest complexes of CDs.[12] However, because of their relatively larger size and numerous atoms, most of these investigations are performed only at the economically viable levels viz. molecular mechanics (MM),[13] molecular dynamics (MD),[14] and Monte Carlo simulations (MC).[15] Recently, the complexation patterns of di- and trivinyl monomers with *β*-CDs and further oligomerization have been systematically analyzed using experimental and computational procedures.[16] Ab initio quantum chemistry calculations are prohibitively expensive to carry out studies on the inclusion complexes of CDs, so an alternative approach is semiempirical methods such as CNDO, AM1, and PM3 methods.[17−23] Few articles are reported on the hydration of α- and *β*-CDs using molecular dynamics simulations.[24] Recently, Raffaini et al. reported the hydration of α-, *β*-, *γ*-, and *δ*-CDs using molecular dynamics simulation methods.[24a] In the present work, inclusion complexes of H_2O, NH_3, NH_4^+, C_6H_6, and bisimidazolyl compounds with α-, *β*-, and *γ*-CDs are studied using quantum mechanical and molecular dynamics simulation methods. The stoichiometry of complexes in both of these methods has been compared, and validation of conformations has been carried out with the available experimental crystal structures. Our interest is to examine the interaction energies of guest molecules with α-, *β*-, and *γ*-CDs.

Computational Methods

Conformational Search. A conformational search was done for ligand molecules (Scheme 1) using the Monte Carlo multiple minimum (MCMM) method as implemented in Macro Model v 9.0 (module of Schrodinger software[25a]) with MM2* force field. The parameters used in the conformational search are the maximum number of steps (5000), the maximum number of iterations (1000), and the gradient (0.001). From the range of conformations that are generated, 10 minimum energy conformations are selected that have maximum and minimum end-

* Corrresponding author. E-mail: gnsastry@yahoo.com.

10.1021/jp9039308 CCC: $40.75
Published on Web 08/05/2009

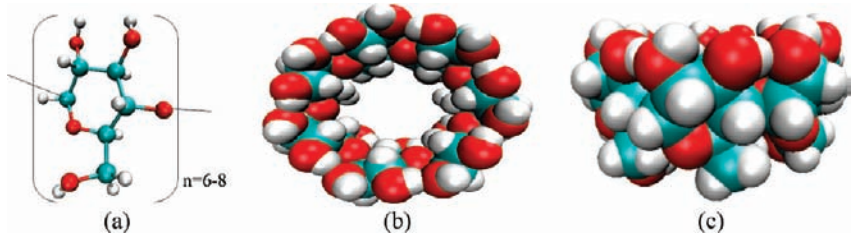

Figure 1. (a) Glucose units linked at the 1,4 position in cyclic fashion (six, seven, and eight for α-, β-, and γ-CDs, respectively). (b) Top view of β-CD. (c) Side view of β-CD.

SCHEME 1: Systems Considered in the Present Study

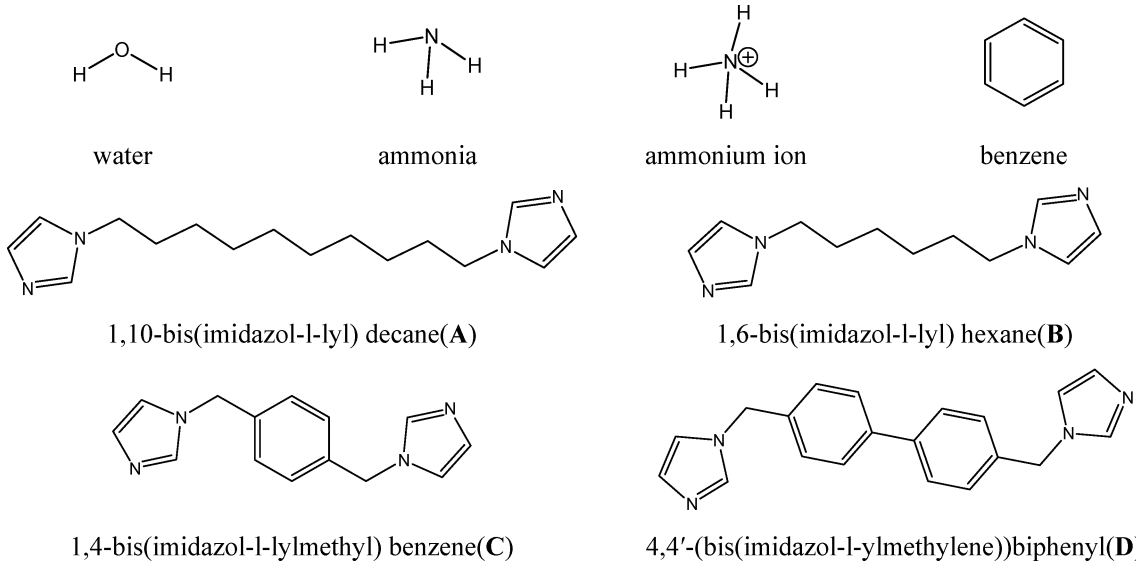

SCHEME 2: Relative Position between the Guest and Cyclodextrin

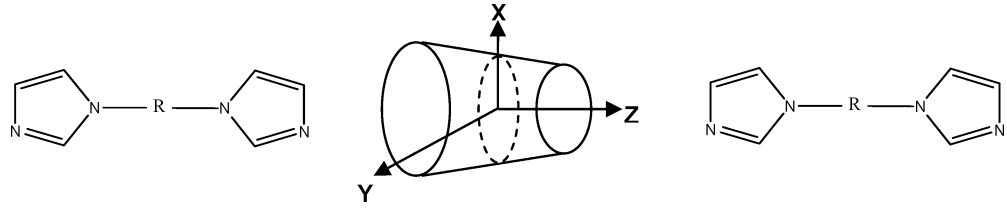

to-end distances for each of the molecules considered. These conformations are optimized at the AM1, PM3, and B3LYP/6-31G levels of theory. Conformations having maximum end-to-end distances (stretched conformation) obtained from the MM2* force field are used for the complex formation and are described in the following section.

Complex Formation. Stretched conformations obtained from the conformational search were taken for making complexes with CDs. Crystal structures of CDs are taken from the Cambridge Structure Database (CSD) and optimized using the PM3 level of theory. The glycosidic oxygen atoms of CD were placed onto the *XY* plane, and the centers of all atoms were defined as the centroid of the CD using Sybyl v 6.9 programs. In the case of the ligand, the center of heavy atoms is defined as the centroid of the ligand. The primary hydroxyl groups of CD were pointed toward the positive direction of the *Z* axis. The longer dimension of the guest molecule was initially placed onto the *Z* axis, and the relative position between the host and the guest was measured by the distance between the centroids of the host and guest molecules. (The schematic representation of the complex formation is shown in Scheme 2.) In the 1:1 complex formation, the ligand enters from the secondary hydroxyl group of CD, where the initial distance between the centroids of the ligand and that of the CDs is kept at 16.0 Å, the distances are changed with a 2.0 Å interval (i.e., 16.0, 14.0, 12.0, 10.0, 8.0, 6.0, 4.0, 2.0, 0.0, −2.0, −4.0, −6.0, −8.0, −10.0, −12.0, −14.0, and −16.0 Å), and the ligand leaves from the primary hydroxyl group. All complexes are optimized at the PM3 level of theory, setting constraints with oxygen atom connecting to sugar units. The constraints are applied such that after optimization, the distances between the centroid of the ligand and the CD vary within a range of ±0.5 Å. All calculations are performed with the Gaussian 03 suite of programs.[25b] In the case of 1:2 complex formations, three orientations between CD units, head-to-head (HH), head-to-tail (HT), and tail-to-tail (TT), have been studied. The distances between the centroids of the two CDs are retained as 16.0, 12.0, and 8.0 Å, respectively. The systems considered in the present study are H_2O, NH_3, NH_4^+, C_6H_6, 1,10-bis(imidazol-l-lyl) decane (**A**), 1,6-bis(imidazol-l-lyl) hexane (**B**), 1,4-bis(imidazol-l-lylmethyl) benzene (**C**), and 4,4′-(bis(imidazol-l-ylmethylene))biphenyl (**D**) (Scheme 1).

Interaction Energy. The interaction energy (IE) is calculated at the PM3 level of theory using eq 1. Monomer (CD and ligands) energies are obtained from the same complex.

$$\Delta E_{int} = E_{com(1:1/1:2)} - E_{CD} - E_{ligand} \quad (1)$$

where ΔE_{int} is the interaction energy, $E_{com(1:1/1:2)}$ is the complex energy in 1:1 or 1:2 stoichiometry, E_{CD} is the CD energy, and E_{ligand} is the ligand energy.

Molecular Dynamics Simulations. The force fields for α-, β-, and γ-CD molecules were taken from the glycam04 force field.[26a] In the case of ligand molecules, bcc charges were applied, and force field parameters were taken from the generalized force field of Wang et al.;[26b] we accomplish the assignment for both bcc charges and atomic force field parameters by using the ANTECHAMBER module of the AMBER 8.0 program.[27] The complex was solvated with the TIP3P water model using a buffer radius of 10.0 Å. The system was minimized to 300 steps using the steepest-descent method, followed by 700 steps of conjugate-gradient minimization, and it was equilibrated to 500 ps time scale by gradual heating to 300 K. The production run was carried out for 1000 ps time scale, and conformations were saved every 10 ps. During equilibration and production dynamics, long-range interactions were treated using the particle mesh ewald (PME) method. The PME charge grid spacing was ~1.0 Å, and the charge grid was interpolated using a cubic B-spline of fourth order, a direct sum tolerance of 0.00001, and 8 Å direct space cutoff. Constant temperature and pressure were maintained throughout the simulations using the Berendsen scaling algorithm[28] with a time constant of 1.0 ps. All bond lengths were constrained using the SHAKE algorithm. A time step of 1.0 fs was used to integrate the equations of motion. All calculations were done with the AMBER 8.0 program.

Calculation of Interaction Energies. The IE of the host−guest complex was calculated using the molecular mechanics Poisson−Boltzmann surface area (MM/PBSA) method.[29] The IE was estimated from free energies of three reactants

$$\Delta G_{bind} = G(RL) - G(R) - G(L) \quad (2)$$

where R is cyclodextrin, L is ligand, and RL is complex.

The relative free energy of each of the reactants is estimated to be the sum of three terms

$$G = \langle E_{MM} \rangle + \langle G_{nes} \rangle + \langle G_{es} \rangle \quad (3)$$

where $\langle G_{nes} \rangle$ is the average hydrophobic contribution to the solvation free energy, $\langle G_{es} \rangle$ is the average electrostatic contribution to the solvation free energy calculated by the solution of Poisson−Boltzmann (PB), and $\langle E_{MM} \rangle$ is the average MM energy of the molecule. The MM energy is the sum of the internal energy of the molecule (i.e., bonded terms, E_{val}) and the electrostatics (E_{ele}) and van der Waals interactions (E_{vdw})

$$E_{MM} = E_{ele} + E_{val} + E_{vdw} \quad (4)$$

All terms in eq 3 are averages of energies obtained from a number of snapshots taken from MD simulations, and ΔG_{bind} values of the ligand−CD complexes were calculated according to eqs 2−4 for all snapshots. The energies were automatically obtained using the MM/PBSA module of the AMBER 8.0 program.

Results and Discussion

In this section, the crystal structure analysis of CDs is first discussed, followed by the conformational analysis of the bisimidazolyl compounds at various levels of theory. Later, semiempirical SCF calculations were carried out on host−guest complexes, where guest molecules are $(H_2O)_n$, $(NH_3)_n$ (n = 1 to 10), $(C_6H_6)_m$ (m = 1 to 6), NH_4^+, and bisimidazolyl compounds. The sequential addition of guest molecules was undertaken to assess the small molecule uptake ability of the cyclodextrins. Obviously, the complexation is solely due to the existence of noncovalent interactions, and when a multitude of noncovalent interactions simultaneously operate, they mutually influence each other.[30] Finally, we discuss the MD simulations of host−guest complexes where guest molecules are C_6H_6 and bisimidazolyl compounds. A total of 357 crystal structures of CDs are available in the Cambridge Structural Database (CSD v.5.28); out of these, α-CD (112), β-CD (214), γ-CD (22), and remaining structures belong to 9-member rings (1), 10-member rings (5), and 14-member rings (3). Here we considered nonmodified CD complexes in which 69 structures belong to α-CD, and 214 and 10 structures belong to β- and γ-CDs, respectively. The rmsd of all crystal structures falls within the 1.0 Å range with respect to crystal structure CSD-IDs BANXUJ, POBRON01, and CIVVMIE10 as references for α-, β-, and γ-CDs, respectively (Figure S1a in the Supporting Information). Diameters of CDs (α-, β-, and γ-CDs) are calculated with respect to heavy atoms at various levels of theory (AM1, PM3, HF/3-21G, and B3LYP/3-21G methods). This study suggests that diameters at the PM3 method are close to experimental values, and the rmsd's of optimized geometries are within 1.30 Å (Figure S1b in the Supporting Information) for α-, β-, and γ-CDs, whereas the rmsd is 2.14 Å for γ-CD at the PM3 level of theory with respect to the crystal structure (CIVVMIE10).

Conformational Search. Conformational analyses performed for **A**, **B**, **C**, and **D** are described in the Computational Methods section. Molecular mechanics force field, semiempirical, Hartree−Fock (HF/6-31G), and density functional methods (B3LYP/6-31G) indicate that stretched conformation is more stable than bent conformation for **A**, **B**, **C**, and **D** (Figure S2 in the Supporting Information). The relative energies are 4 to 6 and 2 to 3 kcal/mol for **A** and **B**, respectively, at the B3LYP/6-31G level of theory. In the case of **C** and **D**, relative energies are in the range of 1 to 2 kcal/mol. In end-to-end distance calculations, the fourth C atom of imidazole is taken to be the reference point. Because the stretched conformation is more stable in all ligands considered in the series, we venture to study both 1:1 (ligand: CD) and 1:2 inclusion complexes. It may easily be expected that the formation of the 1:2 complex is geometrically unviable for the bent conformation.

Semiempirical Methods on Host−Guest Complexes. *$(H_2O)_n$−CD Complexes.* The initial H_2O−CD complex contains 10 water molecules and is optimized at the PM3 level of theory; from this complex, the lowest-energy $(H_2O)_9$−CD complex was obtained by the removal of one water molecule. The total possible conformations are 10, optimized at the PM3 level of theory. The lowest−energy complex, $(H_2O)_9$−CD, was considered to be the starting complex for preparing the $(H_2O)_8$−CD complex and was optimized. Similarly, complexes from $(H_2O)_8$−CD to H_2O−CD were obtained. As shown in Figure 2a, the IE of complexes increases with increasing number of water molecules (conformations are shown in Figure S3 of the Supporting Information). The interaction energy of $(H_2O)_n$-α-CD complexes is greater than that of $(H_2O)_n$-β-CD and $(H_2O)_n$-γ-CD complexes. The IE increases dramatically (4−6 kcal/mol)

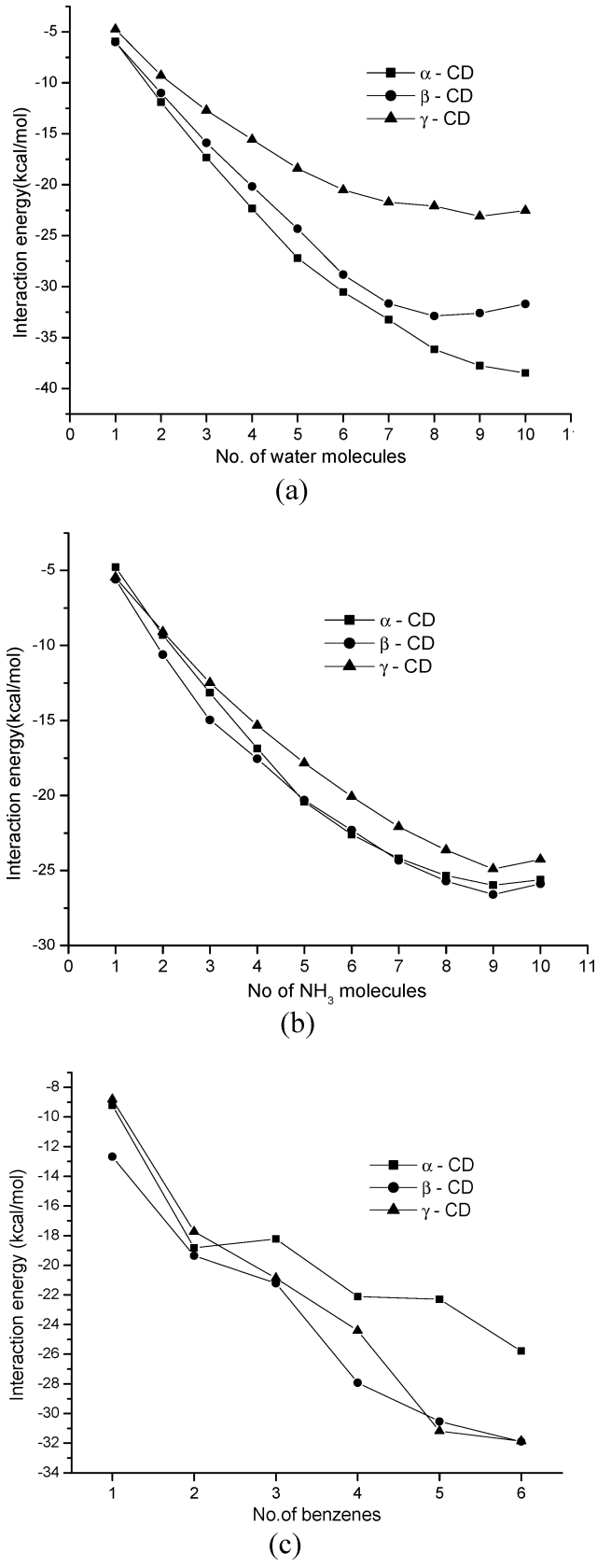

Figure 2. Interaction energy of CDs with increasing number of (a) H_2O molecules, (b) NH_3 molecules, and (c) C_6H_6 molecules.

for each addition of water molecule until the number of water molecules reaches 6; later on, with the addition of each water molecule, IE increases slowly (2 to 3 kcal/mol). Ganazzoli et al., discussed the statistical distribution of the water molecules within the cavity of CDs using the MD simulation method.[25] In the present study, the number of water molecules in the CD cavity is in good agreement with experimental and previous existing results.[25,31]

$(NH_3)_n$−CD Complexes. Figure 2b shows the variation of IE in $(NH_3)_n$−CD complexes with increasing number of NH_3 molecules (n = 1 to 10). The IE is very close in the case of $(NH_3)_n$−α-CD and $(NH_3)_n$-β-CD complexes as compared with $(NH_3)_n$−γ-CD complexes. The IE increases dramatically (3−5 kcal/mol) for each addition of NH_3 molecule until 5 NH_3 molecules are added; later on, with the addition of each NH_3 molecule, IE gradually increases (2 to 3 kcal/mol). The distribution of NH_3 molecules in the CD cavity is two, five, and six molecules for α-, β-, and γ-CDs, respectively (Figure S4 in the Supporting Information).

$(C_6H_6)_n$−CD Complexes. Figure 2c shows the variation of IE in $(C_6H_6)_n$−CD complexes with increasing number of C_6H_6 molecules (n = 1 to 6). Two benzene molecules can be accommodated in the cavity of α-CD, whereas β- and γ-CDs can accommodate three and four benzene molecules in their cavities, respectively (Figure S5 in the Supporting Information). In β-CD, two benzenes are parallel to each other, and the other is perpendicular to these benzenes. In the case of γ-CD complexes, three benzenes are similar to the β-CD complex, whereas the fourth one is in the distorted T-shape in comparison with the remaining three benzenes.

Host−Guest Complexes in 1:1/1:2 Stoichiometry Ratios. ***NH_4^+−CD Complexes.*** Figure 3a shows the disparity of the IE with distance in the host−guest complexes. As expected, the IE of the complex increases as the guest molecule enters the CD cavity and again decreases as the guest exits from the other side of the cavity. In the case of α-CD, NH_4^+ forms a more stable complex with the secondary hydroxyl group as compared with the primary hydroxyl group, but β- and γ-CDs form more stable complexes with primary hydroxyl groups. The IEs are −37.25, −42.74, and −21.79 kcal/mol for α-, β-, and γ-CDs, respectively, at the PM3 level of theory (Figure 4). The IE of NH_4^+ with CD can be attributed to hydrogen bond (H-bond) formation; α-CD forms three H-bonds with secondary hydroxyl groups, whereas β- and γ-CDs form seven and two H-bonds with primary hydroxyl groups, respectively (Figure 4). The average H-bond distances are 2.80, 2.62, and 2.59 Å in α-, β-, and γ-CD complexes, respectively.

A−*CD Complexes.* Figure 3b shows the variation of IEs versus distances for **A**-CD complexes. In 1:1 complexation, IEs are −15 to −22 kcal/mol for α- and β-CD complexes, whereas they are −10 to −14 kcal/mol for the γ-CD complex. The IE is more toward the secondary hydroxyl group of the CD in α- and β-CDs, whereas it is toward the primary hydroxyl group for γ-CD complexes. The maximum end-to-end distance of **A** is 17.39 Å, which is approximately double the depth of the CD cavity (7.9 ± 0.1 Å). Because the inclusion compound composition critically depends on the type of CDs and physicochemical properties of the involved guest, we further studied 1:2 complexation. By the addition of a second CD, the IE increased −14 to −16 kcal/mol for α-CDs and −4 to −6 kcal/mol for β- and γ-CDs. In these stable complexes (1:2 complexes), CDs are oriented in the HH manner, and the distance between centroids of the CD is around 10−12 Å (Figure 5). In other orientations of the CD such as HT, TT is not favorable for complexation. In β-CD complexes, the N atom of both imidazole rings forms three H-bonds with the primary hydroxyl group; distances are 2.76, 2.49, and 2.57 Å, and angles are 151.4, 173.7, and 170.3°, respectively. In α- and γ-CD complexes, H-bonds

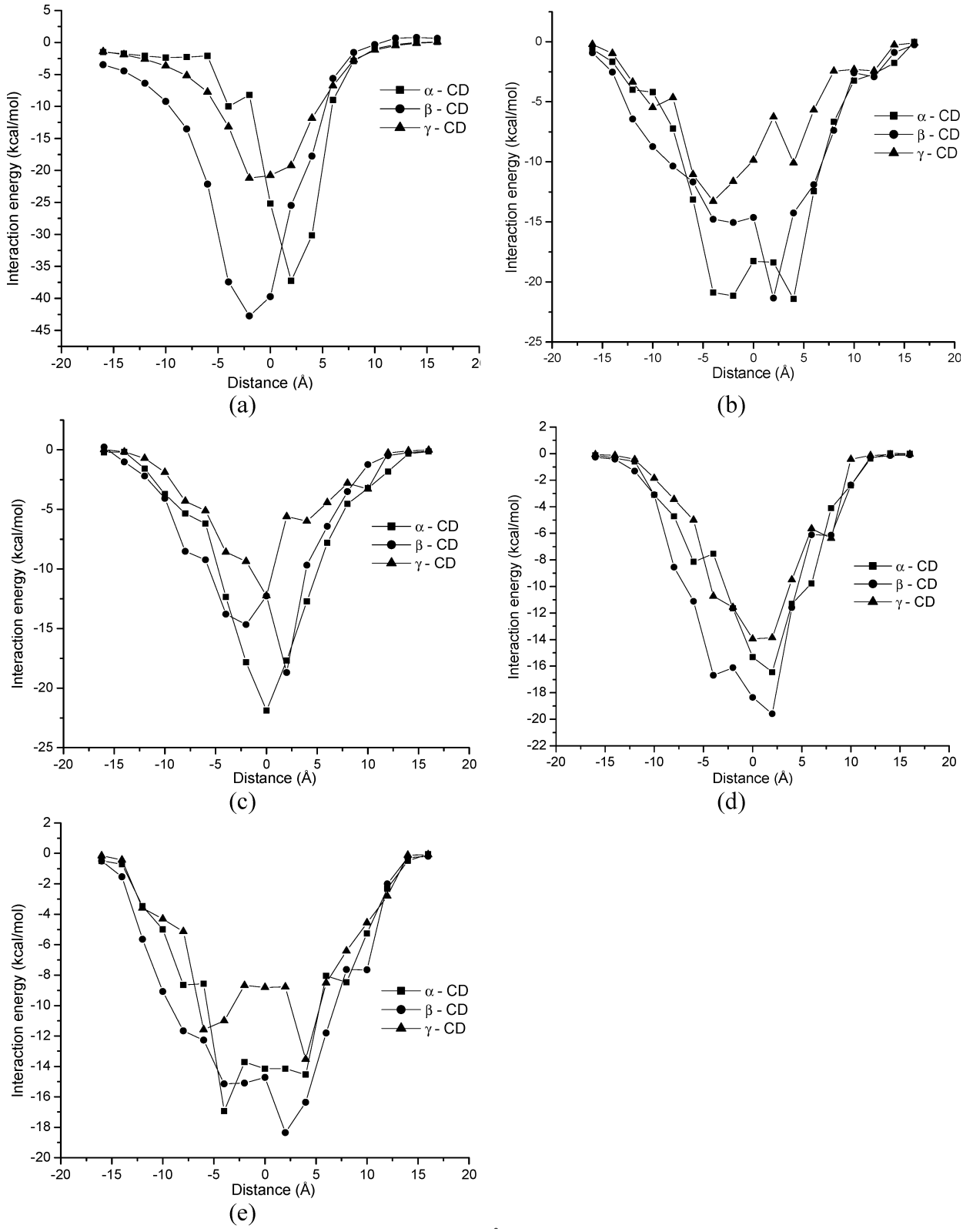

Figure 3. Interaction energy (kilocalories per mole) versus distance (angstroms) in 1:1 stoichiometry complexes obtained at the PM3 level of theory: (a) NH_4^+, (b) **A**, (c) **B**, (d) **C**, and (e) **D**.

are not formed. By considering the IE of 1:1 and 1:2 complexes, **A** prefers to form 1:2 complexes in the HH orientation of CDs.

B−***CD Complexes.*** In the 1:1 complexation, IEs are −21.88, −18.69, and −12.25 kcal/mol for α-, *β*-, and *γ*-CDs, respectively, at the PM3 level of theory. Figure 3c shows the variation of the IE of **B** with distance. The IE is more toward the secondary hydroxyl group of the CD in α-, *β*-, and *γ*-CDs. **B** has four fewer carbon atoms than the **A** molecule with a maximum end-to-end distance of 12.71 Å, which is approximately 4 to 5 Å more than the depth of the CD cavity (7.9 ± 0.1 Å). The addition of the second CD does not provide a substantial increase in IE. Figure 4 shows more stable conformations of **B**−CD complexes in the 1:1 stoichiometry ratio. In α- and *β*-CD complexes, one of the imidazole rings is

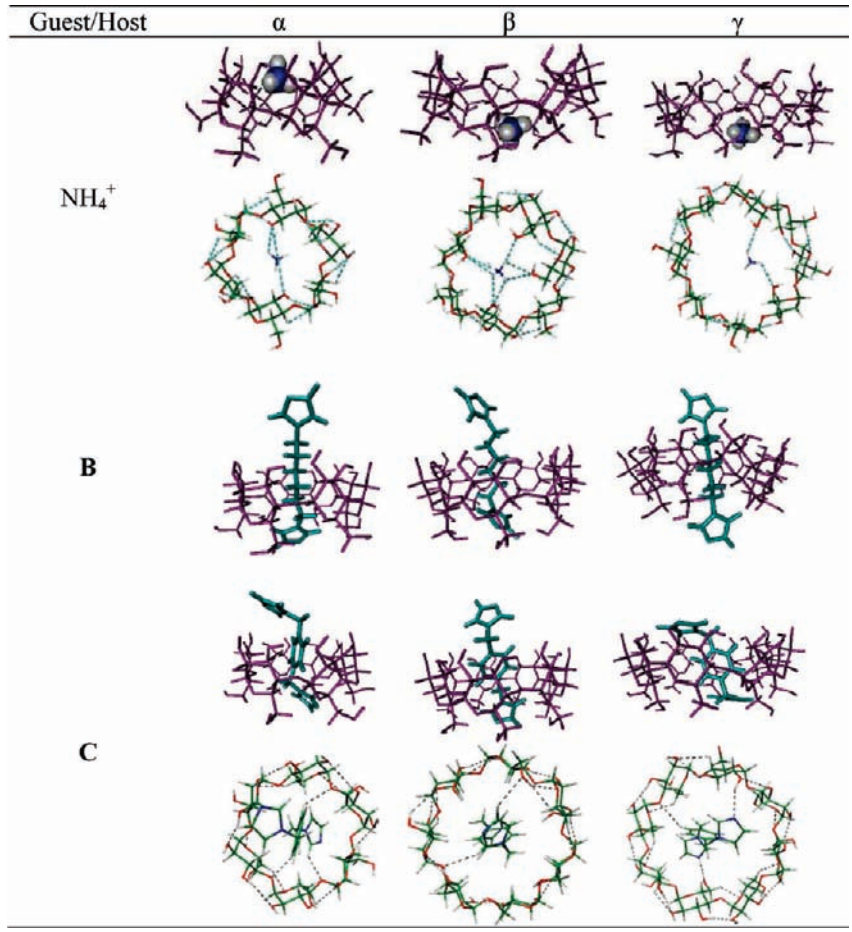

Figure 4. More stable complexes of NH_4^+, **B**, and **C** with α-, *β*-, and *γ*-CDs in the 1:1 stoichiometry ratio obtained at the PM3 level of theory.

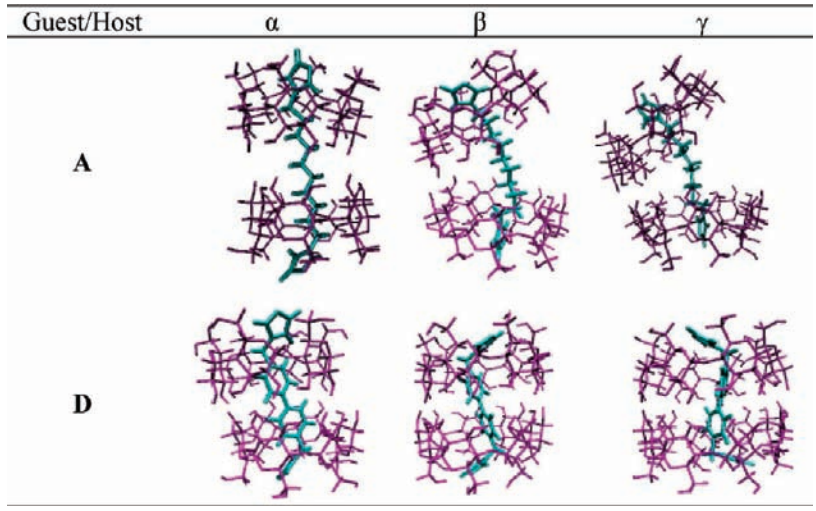

Figure 5. More stable complexes of **A** and **D** with α-, *β*-, and *γ*-CDs in the 1:2 stoichiometry ratio obtained at PM3 level of theory.

in the middle of the CD cavity, whereas for the *γ*-CD complex, the aliphatic chain is in the middle of the cavity. The stability of the complexes can be attributed to H-bond and van der Waals interactions. In the *β*-CD complex, one H-bond is observed between the N atom of imidazole and the primary hydroxyl group of CD; distance and angles are 2.52 Å and 171.4°, respectively, whereas the H-bond is not observed for α- and *γ*-CD complexes. The IE is more for the α-CD complex as compared with that for the *γ*-CD complex. This is due to increased van der Waals interactions in the α-CD complex, which are decreased in *γ*-CD complexes because of the large cavity size. **B** preferentially forms the 1:1 complex rather than 1:2 complexes.

C−*CD Complexes.* Figure 3d shows the variation of the IE with distance between host−guest complexes. The IEs are −16.45, −19.59, and −13.95 kcal/mol for α-, *β*-, and *γ*-CDs, respectively, in the 1:1 complexation (Figure 4). The phenyl ring and one of the imidazole rings is enclosed by the CD cavity for α- and *β*-CDs, and another imidazole ring is present outside of the CD cavity toward the secondary hydroxyl group, whereas

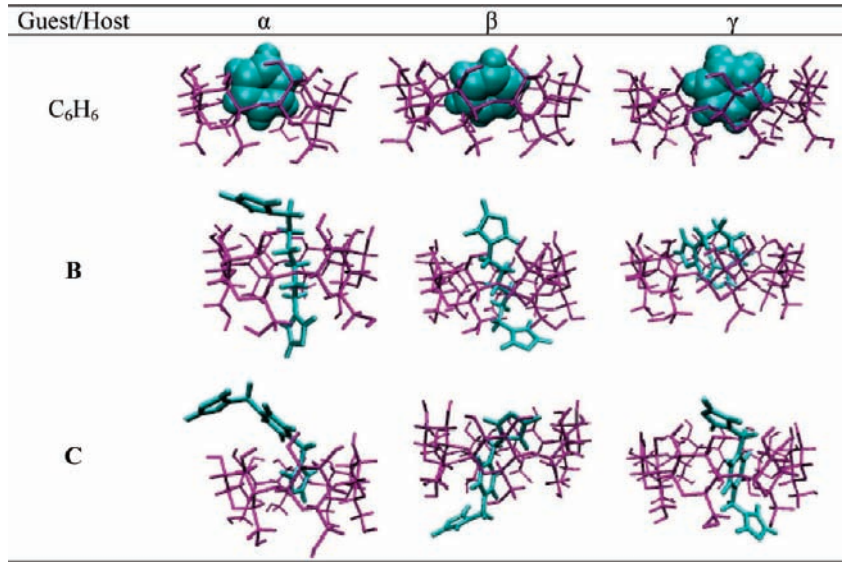

Figure 6. Complexes of C_6H_6, **B**, and **C** with α-, β-, and γ-CDs obtained at 1.0 ns MD simulations in 1:1 stoichiometry ratio.

in the γ-CD complex, both imidazole rings are outside of CD cavity (Figure 4). The IE is more toward the secondary hydroxyl group of the CD as compared with the primary hydroxyl group. The addition of a second CD does not provide a substantial increase in the IE. In the 1:1 complex, α-CD forms three nonconventional H-bonds: one with the second C−H of imidazole and the other two by the phenyl group with the glycosidic oxygen atom of CD (corresponding bond distances 2.96, 2.62, and 2.42 Å and angles 136.6, 130.0, and 142.6°, respectively). In the case of the β-CD complex, two nonconventional H-bonds are observed: one by the fourth C−H of imidazole with the glycosidic oxygen atom of the CD, and the other one is the N atom of the imidazole ring with the primary hydroxyl group of CD (bond distances 2.68 and 2.85 Å and angles 133.6 and 132.5°, respectively (Figure 4)). In the γ-CD complex, three H-bonds are observed in which two are conventional H-bonds formed by the N-atom imidazole with primary and secondary hydroxyl groups and corresponding bond distances of 1.82 and 2.48 Å and angles of 170.5 and 151.1°, respectively. Another one is the nonconventional H-bond between the phenyl group and the glycosidic oxygen atom of CD (2.92 Å, 133.3°). In addition to H-bonds, van der Waals interactions and the size of the CD play a major role in the host−guest complexation, which is observed by the difference in the number of H-bonds among α-, β-, and γ-CD complexes.

D−CD Complexes. Figure 3e shows the IE versus the distance between host−guest complexes in the 1:1 stoichiometry ratio. The IEs are −16.94, −18.35, and −13.53 kcal/mol for α-, β-, and γ-CDs, respectively. The IEs are more toward the secondary hydroxyl group as compared with the primary hydroxyl group. The addition of second CDs provides an increase in the IE in the range of −14 to −16 kcal/mol for α- and β-CDs, whereas it is −7 to −9 kcal/mol for γ-CDs. In these complexes (1:2 complexes), CDs are oriented in the HH manner, and distance between centroids of the CD is around 8−10 Å (Figure 5). Other orientations of CDs such as HT and TT are not favorable for complexation. The N atom of both imidazole rings in α- and β-CD complexes forms three H-bonds with primary hydroxyl groups. The H-bond distances are 2.56, 2.67, and 2.59 Å, and angles are 174.0, 160.4, and 163.7° in the α-CD complex, whereas in the β-CD complex, H-bond distances and angles are 2.59, 2.67, and 2.56 Å and 163.7, 160.4, and 174.0°, respectively. The H-bond is not observed in γ-CD complexes. By considering the IE of CD complexes, **D** prefers to form 1:2 complexes in the HH orientation of CDs.

Molecular Dynamics on Host−Guest Complexes in 1:1/1:2 Ratios. The MD simulations of CD complexes of **A**, **B**, **C**, and **D** in all orientations were studied with 1:1 and 1:2 complexations, whereas benzene was studied with only 1:1 complexation. We studied the complexation of the guest with one CD by considering three initial guest orientations viz. "bottom", "central", and "top". The distance between centroids of the host−guest is −6.0, 0.0, and 6.0 Å in "bottom", "central", and "top", respectively. In 1:2 complexation, three possible orientations, head-to-head (HH), head-to-tail (HT), and tail-to-tail (TT), were studied; the distance between centroids of two CDs is 10−12 Å.

Benzene−CD Complexes. Figure 6 shows the conformations of benzene−CD (α-, β-, and γ-CDs) complexes at 1.0 ns MD simulations. Benzene forms a more stable complex with β-CD as compared with α- and γ-CDs. The IEs are −8.35, −10.17, and −9.06 kcal/mol for α-, β-, and γ-CDs, respectively. The van der Waals interactions play a major role in the complexation of benzene and decrease with increasing size of the CD cavity. Other interactions such as electrostatic and internal energy also have a significant effect on IE, which is greater in the β-CD complex as compared with α- and γ-CDs. In the α-CD complex, the benzene ring is slightly outside of the CD cavity, whereas it is completely covered in the β-CD complex (Figure 6).

A−CD Complexes. The results of the MM/PBSA analysis upon 1.0 ns MD trajectories on three penetration modes of (in 1:1 and 1:2 complexation) complexation are gathered in Table 1 for α-, β-, and γ-CDs, respectively. The IE is −23.50, −19.59, and −18.78 kcal/mol in 1:1 complexation for α-, β-, and γ-CDs, respectively. By the analysis of the MD trajectory, the hydrophobic chain is buried in the CD cavity, whereas both imidazole rings are exposed to the outside of the CD cavity. By the addition of the second CD, the IE increased to 6−8 kcal/mol. The IEs are −28.08, −24.47, and −25.96 kcal/mol for α-, β-, and γ-CDs, respectively, wherein CDs are in the HH orientation (Figure 7). In other orientations, HT and TT IEs are less when compared with those of HH orientations. In HH orientations, the hydrophobic chain and one imidazole ring are buried in the cavity of the CD, whereas the second imidazole ring is exposed from the primary hydroxyl group in α- and β-CDs. In the case of γ-CD, the guest molecule is completely covered by CDs in

TABLE 1: IEs (kilocalories per mole) Obtained with the MM/PBSA Method for the Complexes of A, B, C, and D with α-, *β*-, and *γ*-CDs

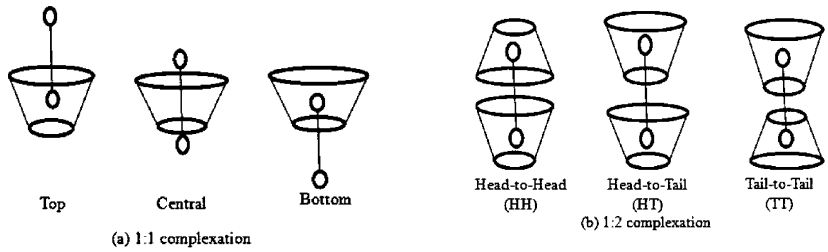

		complexation with one CD			complexation with two CDs		
guest molecules	CD type	central	top	bottom	HH	HT	TT
A	α	−22.28	−23.45	−23.5	−28.08	−26.84	−24.49
	β	−17.82	−19.59	−18.51	−24.47	−19.21	−21.59
	γ	−18.78	−14.72	−18.25	−25.96	−17.64	−21.24
B	α	−21.95	−19.24	−20.63	−21.93	−16.77	−19.6
	β	−10.34	−13.52	−12.96	−13.57	−9.91	−10.02
	γ	−15.07	−15.3	−15.5	−16.47	−13.7	−13.23
C	α	−17.38	−16.01	−16.75	−23.32	−15.26	−18.91
	β	−17.28	−16.5	−15.85	−18.48	−17.37	−17.37
	γ	−17.76	−11.93	−14.12	−16.38	−16.02	−11.77
D	α	−15.97	−9.69	−17.21	−24.97	−22.01	−21.49
	β	−16.79	−14.49	−18.18	−28.11	−13.03	−23.14
	γ	−15.55	−15.3	−16.52	−22.79	−20.24	−20.58

the HH orientation of CDs. In general, the ΔG_{gas} contribution always stabilizes the complex formation by about 25−30 kcal/mol, whereas ($\Delta G_{nes} + \Delta G_{es}$) destabilizes the process by about 15−20 kcal/mol in 1:2 complexes as compared with 1:1 complexes. The electrostatic and van der Waals interactions are important for the complex formation, whereas solvation does not favor complex formation. The IE decreases with increasing size of CD cavity (Table 1) within each considered orientation.

All possible H-bonds formed between primary and secondary hydroxyl groups of CD with the N atom of the imidazole ring were carried out with the help of the PTRAJ subroutine of AMBER. For this N atom to be considered the H-bond acceptor and the OH group of CD to be considered the H-bond donor, a H-bond distance of 3.8 Å and a bond angle of 120° criteria were applied. Here we have analyzed H-bonds on 1:2 complexes of all three orientations of CD. In the case of α-CD, the primary hydroxyl group forms 7% H-bonds in the HH orientation of CDs, and the secondary hydroxyl group forms 52 and 26% H-bonds in HT and TT orientations of CD, respectively. *β*-CD forms 27% H-bonds with the primary hydroxyl group in the HH orientation, whereas HT and TT orientations form 42% H-bonds with the secondary hydroxyl group, respectively. Hydrogen attached to O2 and O3 (secondary hydroxyl groups) forms 81 and 79% of H-bonds in HH and 25% in TT orientation of *γ*-CD, whereas it is 33% in the HT orientation of *γ*-CDs. From the H-bond analysis, the imidazole ring was more exposed from the primary hydroxyl group in *β*-CD as compared with α- and *γ*-CDs in the HH orientation of CD.

Molecular dynamics simulations and density functional methods reveal that **A** forms a 1:2 complex with α-, *β*-, and *γ*-CDs. Hui-Lan Chen et al. reported the crystal structure (CSD-ID: HAHVES) of **A** with *β*-CD in a 1:2 stoichiometry ratio.[32,33] Conformations of the **A**−*β*-CD complex obtained in the crystal structure, PM3 method, and molecular dynamics simulations are shown in Figure 8.

B−***CD Complexes.*** The IE is −21.95, −13.52, and −15.50 kcal/mol in 1:1 complexation for α-, *β*-, and *γ*-CDs, respectively (Table 1). In all three types of CDs, α-CD forms a more stable complex (5−10 kcal/mol) when compared with *β*- and *γ*-CDs. By observing the MD trajectory, the aliphatic chain is covered by the CD cavity in all types of penetration modes of the guest molecule, and both imidazole rings are outside the CD cavity.

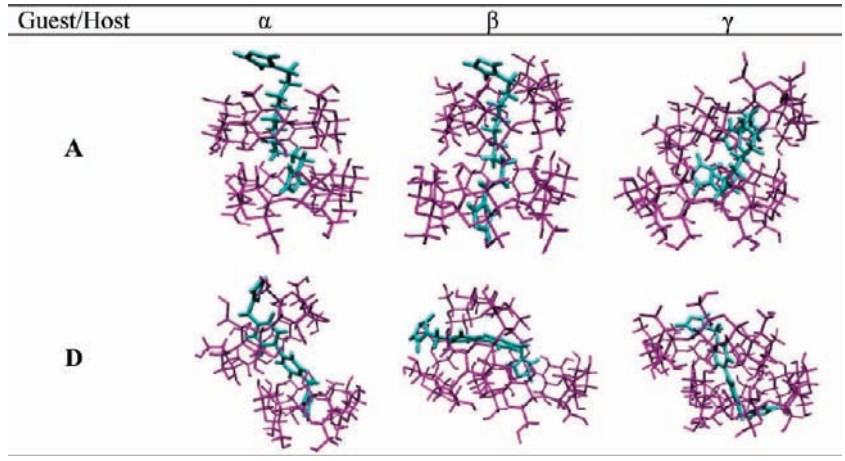

Figure 7. Complexes of **A** and **D** with α-, *β*-, and *γ*-CDs obtained at 1.0 ns MD simulations in 1:2 stoichiometry ratio.

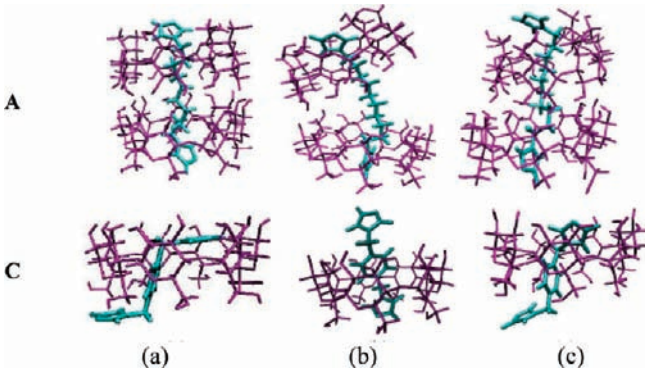

Figure 8. Complexes of **A** and **C** with β-CD obtained in (a) crystal structure, (b) semiempirical methods, and (c) molecular dynamics simulations.

The IE decreases with increasing size of the CD cavity. However, the IE is greater (3.02 kcal/mol) in the γ-CD complex than in the β-CD complex because of the folding of the aliphatic chain of the guest molecule situated properly in the cavity of γ-CD (Figure 6).

By the addition of the second CD, IE does not substantially increase (Table 1). Therefore, **B** prefers to form a 1:1 complex rather than 1:2 complexes. When considering 1:2 complexes, HH orientation is more stable than the other two orientations (HT and TT). By considering three MD runs, primary hydroxyl groups form 6%, whereas secondary hydroxyl groups form 39% of H-bonds in 1:1 complexation of α-CDs. In the case of β-CD, it is 12 and 22%, and in γ-CD, it is 6 and 19% with primary and secondary hydroxyl groups, respectively.

C−*CD Complexes.* Figure 6 shows the conformation obtained at 1.0 ns MD simulations of **C**−CD complexes, and their corresponding IEs are −17.38, −17.28, and −17.76 kcal/mol in 1:1 complexation for α-, β-, and γ-CDs, respectively (Table 1). The addition of the second CD does not provide a substantial increase in the IE in β- and γ-CDs. In the case of α-CD, the addition of a second CD provides 5 to 6 kcal/mol more IE in HH orientations of CDs. The other two orientations (HT and TT) are not favorable for the complexation. In the 1:1 complexation of α-CD, the phenyl group is initially at the bottom, but at the end of equilibration, the phenyl group is capped by CD cavity, which moves toward the secondary hydroxyl group at the end of 1.0 ns time scale in production dynamics (Figure 6). In both "top" and "central" orientations, complexation was observed toward the secondary hydroxyl group. In the case of β- and γ-CDs, the phenyl group is covered by the CD cavity, and both imidazole rings are exposed to the exterior of the CD cavity, in which the imidazole ring toward the primary hydroxyl group is more exposed compared with the secondary hydroxyl group of CD (Figure 6).

In the 1:1 complexation, the average H-bond is 24 and 5% with secondary and primary hydroxyl groups, respectively, for α-CD complexation, whereas it is 28 and 11% for β-CD and 23 and 16% for γ-CD, respectively. In 1:2 complexation of α-CD, the percentage of the H-bond decreased to 16% toward the primary hydroxyl group in the HH orientation of CDs. **C** prefers to form 1:1 complexes with β- and γ-CDs, whereas α-CD forms 1:2 complexes in the HH orientation of CDs.

Hui-Lan Chen et al. reported the crystal structure (CSD-ID: HAHVIW) of **C** with β-CD in the 1:1 stoichiometry ratio.[32,33] Molecular dynamics simulations and semiempirical methods reveal that **C** forms 1:1 complexes with α-, β-, and γ-CDs. Conformations of the **C**−β-CD complex obtained in the crystal structure, PM3 methods, and molecular dynamics simulations are shown in Figure 8.

D−*CD Complexes.* The IE is −17.21, −18.18, and −16.52 kcal/mol in the 1:1 complexation for α-, β-, and γ-CDs, respectively (Table 1). By the analysis of the MD trajectory, it is deduced that the phenyl group is enclosed in the CD cavity, whereas both imidazole rings are exposed to the exterior of the CD cavity. By the addition of the second CD, the IE increased to 8−12 kcal/mol. The IE is −24.97, −28.11, and −22.77 kcal/mol for α-, β-, and γ-CDs, respectively, wherein CDs are in the HH orientation. In other orientations, HT and TT IEs are less when compared with HH orientations (Table 1). In the HH orientation, the phenyl group and one imidazole ring are buried in the CD cavity, whereas the second imidazole ring is exposed to the primary hydroxyl groups of CDs (Figure 7). The ΔG_{gas} contribution stabilizes the complex formation by about 30−40 kcal/mol, whereas ($\Delta G_{nes} + \Delta G_{es}$) destabilizes the process by about 20−25 kcal/mol in 1:2 complexes as compared with that in 1:1 complexes. The IE is more in β-CD by 3 to 4 kcal/mol when compared with α- and γ-CDs.

H-bonds are analyzed on 1:2 complexes in HH orientations of CD. In the case of α-CD, the primary hydroxyl group forms 5% H-bonds in the HH orientation of CDs, whereas it is 44 and 53% for β- and γ-CDs complexes, respectively.

Conclusions

This article provides the stoichiometry of complexes and the interaction energy of guest molecules (H_2O, NH_3, NH_4^+, C_6H_6, and bisimidazolyl compounds) with α-, β-, and γ-CDs by using quantum mechanics and molecular dynamics simulation methods. The following conclusions were drawn from the current study. (1) The diameters of CD with respect to heavy atoms at the AM1, PM3, HF/3-21G, and B3LYP/3-21G levels of theory close to the experimental values. The rmsd of optimized geometries are within 1.30 Å for α- and β-CDs at the PM3 level of theory, but for γ-CD, it is 2.14 Å at the PM3 level of theory with respect to the crystal structure (CIVVMIE10). (2) From the CSD database, the rmsd of the unmodified crystal structures falls within the 1.0 Å range with respect to crystal structure CSD-IDs BANXUJ, POBRON01, and CIVVMIE10 as reference for the α-, β-, and γ-CDs, respectively. (3) The IE increases dramatically (4−6 kcal/mol) for each addition of water molecule until the number of water molecules reaches six; later on, with the addition of each water molecule, the IE slowly increases (2 to 3 kcal/mol). The cavity of the CD is occupied by three, seven, and nine water molecules for α-, β-, and γ-CDs, respectively. (4) The distribution of the NH_3 molecule in the cavity of CDs is two, five, and six molecules for α-, β-, and γ-CDs, respectively. Two benzene molecules can be accommodated in the α-CD cavity, whereas β- and γ-CDs can accommodate three and four benzene molecules, respectively. (5) The guest molecule, NH_4^+, binds to the secondary hydroxyl group in α-CDs, whereas in β- and γ-CDs, it binds to the primary hydroxyl group. (6) Both quantum and MD simulations show that benzene forms a more stable complex with β-CD as compared with α- and γ-CDs. (7) 1,10-Bis(imidazol-l-lyl) decane (**A**) prefers to form 1:2 complexes with α-, β-, and γ-CDs in the HH orientation of CDs, wherein α-CD forms a more stable complex. (8) 1,6-Bis(imidazol-l-lyl) hexane (**B**) forms a 1:1 complex with all three types of CDs; among these, α-CD forms a more stable complex. (9) 1,4-Bis(imidazol-l-lylmethyl) benzene (**C**) forms 1:2 complexes with α-CDs, whereas it forms a 1:1 complex with β- and γ-CDs. In the 1:1 complexation, the β-CD complex is more stable than α- and

γ-CDs. (10) 4,4′-(Bis(imidazol-l-ylmethylene))biphenyl (**D**) prefers to form 1:2 complexes with α-, β-, and γ-CDs in the HH orientation of CDs, wherein β-CD forms a more stable complex. The conformation obtained from quantum and MD simulation methods has good correlations with crystal conformations (**A** and **C** complexes).

Acknowledgment. We thank DST for financial support in the form of the Swarna Jayanthi Fellowship grant. M.N. thanks CSIR for financial assistance.

Supporting Information Available: Interaction energy of guest molecules (H_2O, NH_3, NH_4^+, C_6H_6, and bisimidazolyl) with CDs (α-, β-, and γ-CDs) at the PM3 level of theory. Conformation obtained at 1.0 ns MD simulations and various energy components obtained in MM/PBSA analysis. This material is available free of charge via the Internet at http://pubs.acs.org.

References and Notes

(1) Lehn, J. M. *Angew. Chem., Int. Ed. Engl.* **1988**, *27*, 90.
(2) Cram, D. J. *Angew. Chem., Int. Ed. Engl.* **1988**, *27*, 1009.
(3) Freudenberg, K.; Plankenhorn, E.; Knauber, H. *Chem. Ind.* **1947**, 731.
(4) (a) Szejtli, J. *Chem. Rev.* **1998**, *98*, 1743. (b) D'Souza, V. T.; Lipkowitz, K. B. *Chem. Rev.* **1998**, *98*, 1741. (c) Uekama, K.; Hirayama, F.; Irie, T. *Chem. Rev.* **1998**, *98*, 2045. (d) Schneider, H. J.; Hacket, F.; Rudiger, V.; Ikeda, H. *Chem. Rev.* **1998**, *98*, 1755. (e) Takahashi, K. *Chem. Rev.* **1998**, *98*, 2013. (f) Khan, A. R.; Forgo, P.; Stine, K. J.; D'Souza, V. T. *Chem. Rev.* **1998**, *98*, 1977.
(5) (a) Nepogodiev, S. A.; Stoddart, J. F. *Chem. Rev.* **1998**, *98*, 1959. (b) Gerhard, W.; Bao-Hang, H.; Axel, M. *Chem. Rev.* **2006**, *106*, 782. (c) Harada, A. *Acc. Chem. Res.* **2001**, *34*, 456. (d) Kim, B.; Hong, J. *Chem. Lett.* **2002**, 336. (e) Buston, J. E. H.; Young, J. R.; Anderson, H. L. *Chem. Commun.* **2000**, 905. (f) Eliadou, K.; Yannakopoulou, K.; Rontoyianni, A.; Mavridis, I. M. *J. Org. Chem.* **1999**, *64*, 6217–6226.
(6) VanEtten, R. L.; Sebastian, J. F.; Glowes, G. A.; Bender, M. L. *J. Am. Chem. Soc.* **1967**, *89*, 3242.
(7) Tabushi, I.; Yamamura, K.; Fujita, K.; Kawakubo, H. *J. Am. Chem. Soc.* **1979**, *101*, 1019.
(8) Cramer, F.; Saenger, W.; Spatz, H. Ch. *J. Am. Chem. Soc.* **1967**, *89*, 14.
(9) Kondo, H.; Nakatani, H.; Hiromi, K. *J. Biochem.* **1976**, *79*, 393.
(10) Ueno, A.; Yoshimura, H.; Saka, R.; Osa, T. *J. Am. Chem. Soc.* **1979**, *101*, 2779.
(11) Odagaki, Y.; Hirotsu, K.; Higuchi, T.; Harada, A.; Takahashi, S. *J. Chem. Soc., Perkin Trans.* **1990**, *1*, 1230.
(12) Lindner, K.; Saenger, W. *Carbohydr. Res.* **1982**, *99*, 103.
(13) (a) Lipkowitz, K. B. *Chem. Rev.* **1998**, *98*, 1829. (b) Liu, L.; Guo, Q. X. *J. Phys. Chem. B* **1999**, *103*, 3461.
(14) (a) Bonnet, P.; Jaime, C.; Morin-Allory, L. *J. Org. Chem.* **2001**, *66*, 689. (b) Bea, I.; Gotsev, M. G.; Ivanov, P. M.; Jaime, C.; Kollman, P. A. *J. Org. Chem.* **2006**, *71*, 2056. (c) Thomson, D.; Larsson, J. A. *J. Phys. Chem. B* **2006**, *110*, 16640. (d) Carlos-Javier, N. A.; Carolina-Marta, E. L.; David, D.; Carlos, J.; Ramon, G. J. *Tetrahedron* **2006**, *62*, 4162.
(15) (a) Grabner, G.; Monti, S.; Mayer, B.; Koehler, G. *J. Phys. Chem.* **1996**, *100*, 20068. (b) Tanaka, H.; Kato, N.; Kawazura, H. *Bull. Chem. Soc. Jpn.* **1997**, *70*, 1255.
(16) (a) Sunita, S. S.; Rohini, N. K.; Kulkarni, M. G.; Nagaraju, M.; Sastry, G. N. *J. Am. Chem. Soc.* **2006**, *128*, 7752. (b) Sunita, S. S.; Rohini, N. K.; Kulkarni, M. G.; Nagaraju, M.; Sastry, G. N. *Macromolecules* **2007**, *40*, 1824.
(17) Kitagawa, M.; Hoshi, H.; Sakurai, M.; Inoue, Y.; Chûjô, R. *Carbohydr. Res.* **1987**, *163*, c1.
(18) Bosti, A.; Yannakopoulou, K.; Hadjoudis, E.; Waite, J. *Carbohydr. Res.* **1996**, *283*, 1.
(19) (a) Huang, M. J.; Watts, J. D.; Bodor, N. *Int. J. Quantum Chem.* **1997**, *64*, 711. (b) Huang, M. J.; Watts, J. D.; Bodor, N. *Int. J. Quantum Chem.* **1997**, *65*, 1135.
(20) Castro, R.; Berardi, M. J.; Cordova, E.; de Olza, M. O.; Kaifer, A. E.; Evanseck, J. D. *J. Am. Chem. Soc.* **1996**, *118*, 10257.
(21) Li, X. S.; Liu, L.; Guo, Q. X.; Chu, S. D.; Liu, Y. C. *Chem. Phys. Lett.* **1999**, *307*, 117.
(22) Song, K. S.; Hou, C. R.; Liu, L.; Li, X. S.; Guo, Q. X. *J. Photochem. Photobiol., A* **2001**, *139*, 105.
(23) (a) Santos, H. F. D.; Duarte, H. A.; Sinisterra, R. D.; Mattos, S. V. D. M.; Oliveira, L. F. C. D.; Almeida, W. B. D. *Chem. Phys. Lett.* **2000**, *319*, 569. (b) Jursic, B. S.; Zdravkovski, Z.; French, A. D. *THEOCHEM* **1996**, *366*, 113.
(24) (a) Raffaini, G.; Ganazzolo, F. *Chem. Phys.* **2007**, *333*, 128. (b) Georg, C. H.; Coutinho, K.; Canuto, S. *Chem. Phys. Lett.* **2005**, *413*, 16. (c) Naidoo, J. K.; Chen, J. Y.; Jansson, J. L. M.; Widmalm, G.; Maliniak, A. *J. Phys. Chem. B* **2004**, *108*, 4236. (d) Winkler, R. G.; Fioravanti, S.; Ciccotti, G.; Margheritis, C.; Villa, M. *J. Comput.-Aided Mol. Des.* **2000**, *14*, 659.
(25) (a) *Macro Model*, version 9.0; Schrodinger, LLC: New York, 2007. (b) Frisch, M. J.; Trucks, G. W.; Schlegel, H. B.; Scuseria, G. E.; Robb, M. A.; Cheeseman, J. R.; Montgomery, J. A., Jr.; Vreven, T.; Kudin, K. N.; Burant, J. C.; Millam, J. M.; Iyengar, S. S.; Tomasi, J.; Barone, V.; Mennucci, B.; Cossi, M.; Scalmani, G.; Rega, N.; Petersson, G. A.; Nakatsuji, H.; Hada, M.; Ehara, M.; Toyota, K.; Fukuda, R.; Hasegawa, J.; Ishida, M.; Nakajima, T.; Honda, Y.; Kitao, O.; Nakai, H.; Klene, M.; Li, X.; Knox, J. E.; Hratchian, H. P.; Cross, J. B.; Adamo, C.; Jaramillo, J.; Gomperts, R.; Stratmann, R. E.; Yazyev, O.; Austin, A. J.; Cammi, R.; Pomelli, C.; Ochterski, J. W.; Ayala, P. Y.; Morokuma, K.; Voth, G. A.; Salvador, P.; Dannenberg, J. J.; Zakrzewski, V. G.; Dapprich, S.; Daniels, A. D.; Strain, M. C.; Farkas, O.; Malick, D. K.; Rabuck, A. D.; Raghavachari, K.; Foresman, J. B.; Ortiz, J. V.; Cui, Q.; Baboul, A. G.; Clifford, S.; Cioslowski, J.; Stefanov, B. B.; Liu, G.; Liashenko, A.; Piskorz, P.; Komaromi, I.; Martin, R. L.; Fox, D. J.; Keith, T.; Al-Laham, M. A.; Peng, C. Y.; Nanayakkara, A.; Challacombe, M.; Gill, P. M. W.; Johnson, B.; Chen, W.; Wong, M. W.; Gonzalez, C.; Pople, J. A. *Gaussian 03*, revision C.1; Gaussian, Inc.: Pittsburgh, PA, 2003.
(26) (a) Kirschner, K. N.; Woods, R. J. *Proc. Natl. Acad. Sci. U.S.A.* **2001**, *98*, 10541. (b) Wang, J.; Wolf, R. M.; Caldwell, J. W.; Kollman, P. A.; Case, D. A. *J. Comput. Chem.* **2004**, *25*, 1157.
(27) Case, D. A.; Pearlman, D. A.; Caldwell, J. W.; Cheatham, T. E., III.; Wang, J.; Ross, W. S.; Simmerling, C. L.; Darden, T. A.; Merz, K. M.; Stanton, R. V.; Cheng, A. L.; Vincent, J. J.; Crowley, M.; Tsui, V.; Gohlke, H.; Radmer, R. J.; Duan, Y.; Pitera, J.; Massava, I.; Seibel, G. L.; Singh, U. C.; Weiner, P. K.; Hornak, V.; Cui, G.; Schafmeister, C.; Gohlke, J.; Kollman, P. A. *AMBER 8.0*; University of California: San Francisco, CA, 2004.
(28) Berendsen, H. J. C.; Postma, J. P. M.; van Gunsteren, W.; DiNola, A.; Haak, J. R. *J. Chem. Phys.* **1984**, *81*, 3684.
(29) Kollman, P. A.; Massova, I.; Reyes, C.; Kuhn, B.; Huo, S.; Chong, L.; Lee, M.; Lee, T.; Duan, Y.; Wang, W.; Donini, O.; Cieplak, P.; Srinivasan, J.; Case, D. A.; Cheatham, T. E. *Acc. Chem. Res.* **2000**, *33*, 889.
(30) (a) Wieczorek, R.; Haskamp, L.; Dannenberg, J. J. *J. Phys. Chem. A* **2004**, *108*, 6713. (b) Kobko, N.; Dannenberg, J. J. *J. Phys. Chem. A* **2003**, *107*, 10389. (c) Vijay, D.; Zipse, H.; Sastry, G. N. *J. Phys. Chem. B* **2008**, *112*, 8863. (d) Reddy, A. S.; Vijay, D.; Sastry, G. M.; Sastry, G. N. *J. Phys. Chem. B* **2006**, *110*, 2479.
(31) (a) Manor, P. C.; Saenger, W. *J. Am. Chem. Soc.* **1974**, *96*, 3630. (b) Betzel, C.; Saenger, W.; Hingerty, B. E.; Brown, G. M. *J. Am. Chem. Soc.* **1984**, *106*, 7545. (c) Ding, J.; Steiner, T.; Zabel, V.; Hingerty, B. E.; Mason, S. A.; Saenger, W. *J. Am. Chem. Soc.* **1991**, *113*, 8081. (d) Fujiwara, T.; Tanaka, N.; Kobayashi, S. *Chem. Lett.* **1990**, 739.
(32) Xu-Jie, S.; Hui-Lan, C.; Fei, Y.; You-Cai, Z.; Xiao-Hong, Y.; Yi-Zhi, Li. *Tetrahedron Lett.* **2004**, *45*, 6813.
(33) Hui-Lan, C.; Zhao, B.; Wang, Z. *J. Inclusion Phenom. Macrocyclic Chem.* **2006**, *56*, 17.

JP9039308